Supplementary Material

Cytosine Methylation Alters DNA Mechanical Properties

Philip M.D. Severin, Xueqing Zou, Hermann E. Gaub and Klaus Schulten

Supporting Methods

MFA DNA-chip (bottom surface)

The DNA-chip (see Fig. 1) has been assembled as described previously (1) except for some modifications. DNA oligomers **1**, **2**, and **3** were purchased HPLC grade from IBA GmbH (Göttingen, Germany) and Metabion GmbH (Martinsried, Germany). Oligonucleotides employed had the following sequences and modifications (methylations, **mC** represents 5-methylcytosine):
$\mathbf{1_{nDNA}}$, NH_2-$(HEGL)_5$-5'-$(T)_{10}$-CCG AGA TAT CCG CAC CAA CG-3';
$\mathbf{2_{nDNA}}$, 3'-GGC TCT ATA GGC GTG GTT GC-$(T)_6$-5'-5'-T(Cy5)-$(T)_6$-GGC TCT ATA GGC GTG GTT GC-3';
$\mathbf{1_{mC-1c-DNA}}$, NH_2-$(HEGL)_5$-5'-$(T)_{10}$-CCG AGA TAT C**mC**G CAC CAA CG-3';
$\mathbf{2_{mC-1c-DNA}}$, 3'-GGC TCT ATA GG**mC** GTG GTT GC-$(T)_6$-5'-5'-T(Cy5)-$(T)_6$-GGC TCT ATA GGC GTG GTT GC-3';
$\mathbf{1_{mC-3-DNA}}$, NH_2-$(HEGL)_5$-5'-$(T)_{10}$-C**mC**G AGA TAT C**mC**G CAC CAA **mC**G-3';
$\mathbf{2_{mC-3-DNA}}$, 3'-GG**mC** TCT ATA GG**mC** GTG GTT G**mC**-$(T)_6$-5'-5'-T(Cy5)-$(T)_6$-GGC TCT ATA GGC GTG GTT GC-3';
$\mathbf{3_{Ref}}$, biotin-5'-$(T)_{10}$-GCA ACC ACG CCT ATA GAG CC(Cy3)-3'.

Oligomers **1** contained five hexaethyleneglycol (HEGL) linkers connected via phosphate groups. The lower duplex **1** • **2** contains zero, one or three 5-methylcytosine (**mC**) per strand. DNA oligomer **1** is amine-modified, which allows covalent linkage to aldehyde-functionalized glass slides (Schott GmbH, Jena, Germany).

We spotted 1 μL drops of 5× SSC (saline sodium citrate; Sigma-Aldrich GmbH, Munich, Germany) containing 25 μM oligomer **1** on the aldehyde slide in a 4×4 pattern and incubated the slide in a saturated NaCl ddH_2O atmosphere overnight. After washing the slide with ddH_2O containing 0.2% sodium dodecyl sulfate (SDS; VWR Scientific GmbH, Darmstadt, Germany) and thoroughly rinsing the slide with ddH2O we reduced the resulting Schiff bases with 1% aqueous $NaBH_4$ (VWR Scientific GmbH, Darmstadt, Germany) for 90 min. Subsequently, the slide was washed with 1× SSC and thoroughly rinsed with ddH_2O.

In order to reduce nonspecific binding, the slides were blocked in 1× SSC containing 4% bovine serum albumin (BSA; Sigma-Aldrich GmbH, Munich, Germany) for 20 min. Custom-made 16-well silicone isolators (Grace-Biolabs, OR) were placed on top of the immobilized DNA oligomer **1**. The 100 nM Cy5-modified oligomer **2** and 200 nM biotin-modified oligomer **3** were hybridized to the latter for 30 min, completing the **1** • **2** • **3** complex on the glass slide (see Fig. 1*a*). After removing the silicone isolators the slides were washed with a self-built fluidic system driven by a multi-channel peristaltic pump (Ismatec GmbH, Wertheim-

Mondfeld, Germany) to remove any unspecific bound DNA oligomers. The 4×4 pattern was rinsed subsequently with 2× SSC, 0.2× SSC containing 0.1% Tween 20 (VWR Scientific GmbH, Darmstadt, Germany) and 1× PBS (phosphate buffered saline) each with 50 ml in 5 min.

MFA PDMS stamp (top surface)

The stamp (see Fig. 1) was made of polydimethylsiloxane (PDMS) and was fabricated and functionalized as described previously (2, 3). Briefly summarized, the PDMS stamps were cut into a 4×4 pillar arrangement. Each pillar is 1 mm in diameter and 1 mm in height, and carries a microstructure on the flat surface; 100 mm×100 mm pads are separated by 41 mm wide and 5 mm deep trenches allowing for liquid drainage during the contact and separation process. Free polymers were extracted in toluene for at least one day (4). The PDMS was activated overnight in 12.5% hydrochloric acid and subsequently derivatized with (3-glycidoxypropyl)-trimethoxysilane (ABCR, Karlsruhe, Germany) to generate epoxide groups. NH_2-PEG-Biotin (3400 g/mol; Rapp Polymere, Tübingen, Germany) was melted at 80°C, and ∼1 mL was spotted on each pillar followed by overnight incubation in argon atmosphere at 80°C. The excess polymers were thoroughly removed with ddH_2O. Shortly before the experiment, the PDMS was incubated for 60 min with 1 mg/mL streptavidin (Thermo Fisher Scientific, Bonn, Germany) that had been dissolved before in 1× PBS and 0.4% BSA. The PDMS was then washed with 1× PBS containing 0.1% Tween 20. Lastly, the PDMS was washed in 1× PBS and gently dried with N_2 gas.

AFM sample and cantilever fuctionalization

For our AFM measurements we employed a commercial instrument (Molecular Force Probe 3D from Asylum Research) with cantilevers from Veeco (MLCT) and Olympus (BL-AC40).

A detailed description of the sample preparation can be found in reference (5). The following oligonucleotides (same sequence of the DNA duplex as in the MFA experiment) modified with a thiol group at their 5'-termini (IBA GmbH, Göttingen, Germany) were immobilized on amino-functionalized surfaces using a hetero-bifunctional poly-ethylene glycol (PEG) spacer (6):
$\mathbf{S_{nDNA}}$, 5'-SH-$(T)_{20}$-CGT TGG TGC GGA TAT CTC GG-3';
$\mathbf{C_{nDNA}}$, 5'-SH-$(T)_{10}$-CCG AGA TAT CCG CAC CAA CG-3';
$\mathbf{S_{mC-1c-DNA}}$, 5'-SH-$(T)_{20}$-CGT TGG TG**mC** GGA TAT CTC GG-3';
$\mathbf{C_{mC-1c-DNA}}$, 5'-SH-$(T)_{10}$-CCG AGA TAT C**mC**G CAC CAA CG-3';
$\mathbf{S_{mC-3-DNA}}$, 5'-SH-$(T)_{20}$-**mC**GT TGG TG**mC** GGA TAT CT**mC** GG-3';
$\mathbf{C_{mC-3-DNA}}$, 5'-SH-$(T)_{10}$-C**mC**G AGA TAT C**mC**G CAC CAA **mC**G-3'.

One type of oligonucleotide ($\mathbf{C_x}$) was immobilized on the cantilever and the oligonucleotide with the complementary sequence was coupled to the surface ($\mathbf{S_x}$), as shown in Fig. 2*a*. Amino-modified surfaces on the cantilevers were prepared using 3-aminopropyldimethylethoxysilane (ABCR GmbH, Karlsruhe, Germany) (7). Commercially available amino-

functionalized slides (Slide A, Nexterion, Mainz, Germany) were used. In the following, both surfaces (cantilever and slide) were treated in parallel as described previously (8). They were incubated at pH 8.5 in borate buffer for 1 h for deprotonation of the amino groups in order to couple the surface to the N-hydroxysuccinimide (NHS) groups of the heterobifunctional NHS-PEG-maleimide (molecular weight, 5000 g/mol; Rapp Polymere, Tübingen, Germany). Subsequently, slide and cantilever were incubated for 1 h in PEG (50 mM) that had been dissolved before in borate buffer at pH 8.5. The oligonucleotides were reduced using tris (2-carboxyethyl) phosphine hydrochloride beads (Perbio Science, Bonn, Germany) to generate free thiols. After washing the surfaces with ddH_2O, a solution of the oligonucleotides (30 μM) was incubated on the surfaces for 1 h (or over night). Before measurement, the surfaces were rinsed with 1× PBS to remove non-covalently bound oligonucleotides and stored in 1× PBS until use.

Simulated systems

DNA of the same sequence as employed in the experiments was studied in molecular dynamics simulations. We investigated three different DNA methylation patterns, namely, non-methylated (nDNA), center-methylated (cDNA) and fully-methylated (fDNA):
nDNA, 5'-CCGAGATATCCGCACCAACG-3',
5'-CGTTGGTGCGGATATCTCGG-3';
cDNA, 5'-CCGAGATATC**mC**GCACCAACG-3',
5'-CGTTGGTG**mC**GGATATCTCGG-3';
fDNA, 5'-C**mC**GAGATATC**mC**GCACCAA**mC**G-3',
5'-**mC**GTTGGTG**mC**GGATATCT**mC**GG-3'.

A double-stranded helix of native DNA was built with the program X3DNA (9). Methylated DNA was generated by altering cytosines to methylated cytosines employing the program psfgen (10). The topology of DNA along with the missing hydrogen atoms were generated also using psfgen (10) with the resulting topology files corresponding to CHARMM27 (11). DNA was placed in a water box of size 300 Å×60 Å×60 Å. 0.1 mol/L KCl was added, amounting to 87 K^+ and 47 Cl^- ions, the difference in ion numbers serving neutralization of DNA. The resulting system is shown in Fig. 3*a*. Each simulated system contained about 110,000 atoms of DNA, water and ions.

Molecuar dynamics simulations

Simulations were performed using NAMD 2.6 (10) with the CHARMM27 force field for DNA (11) and the TIP3P water model (12). Periodic boundary conditions were assumed and the particle mesh Ewald (PME) summation method was employed for evaluating Coulomb forces. The van der Waals (vdW) energy was calculated using a smooth cutoff of 12 Å. The integration time step was 1 fs. The temperature was kept at 310 K by applying Langevin forces (13) with a damping coefficient of 0.1 ps^{-1} only to the oxygen atoms of water molecules.

The system was energy minimized for 2000 steps, then heated to 295 K in 4 ps. To determine the volume leading to a suitable overall density and corresponding to the laboratory pressure, 500 ps-equilibration was conducted under NPT ensemble conditions. This equilibration was performed using Nosé-Hoover Langevin piston pressure control (13). After the system acquired in the NPT ensemble description a constant volume, 2 ns-equilibration was conducted under NVT ensemble conditions.

Supporting Results

Determination of the mechanical stability of mC-1u-DNA and mC-1d-DNA by MFA measurements

We investigated how each mCG-pair, close to the ends of the 20 bp DNA duplex, affects its mechanical stability. For this purpose, two new DNA constructs, mC-1d-DNA and mC-1u-DNA, were examined. Because of cost issues, a simpler construct without a 5'-5'-DNA direction correction was used, i.e., the reference duplex was pulled at the 3'-end, while the target duplex is still pulled at the 5'-end. The following sequences were used (mC represents 5-methylcytosine):
$\mathbf{1_{nDNA}}$, NH_2-$(HEGL)_5$-5'-$(T)_{10}$-CCG AGA TAT CCG CAC CAA CG-3';
$\mathbf{2_{nDNA}}$, 3'-GGC TCT ATA GGC GTG GTT GC-$(T)_6$-T(Cy5)-$(T)_6$-GGC TCT ATA GGC GTG GTT GC-5';
$\mathbf{1_{mC-1u-DNA}}$, NH_2-$(HEGL)_5$-5'-$(T)_{10}$-CCG AGA TAT CCG CAC CAA **mC**G-3';
$\mathbf{2_{mC-1u-DNA}}$, 3'-GGC TCT ATA GGC GTG GTT G**mC**-$(T)_6$-T(Cy5)-$(T)_6$-GGC TCT ATA GGC GTG GTT GC-5';
$\mathbf{1_{mC-1d-DNA}}$, NH_2-$(HEGL)_5$-5'-$(T)_{10}$-C**mC**G AGA TAT CCG CAC CAA CG-3';
$\mathbf{2_{mC-1d-DNA}}$, 3'-GG**mC** TCT ATA GGC GTG GTT GC-$(T)_6$-T(Cy5)-$(T)_6$-GGC TCT ATA GGC GTG GTT GC-5';
$\mathbf{3_{Ref}}$, 5'-(Cy3)-GCA ACC ACG CCT ATA GAG CC-$(T)_{10}$-biotin-3'.

Since we pulled DNA at the 3'-ends of the reference duplex and the pulling direction (3' or 5') on the DNA has an effect on the mechanical stability (14, 15), a direct comparison of the NF values of mC-1c-DNA and mC-3-DNA is not possible. However, not only mC-1u-DNA and mC-1d-DNA, but also nDNA was measured with this reference duplex. This allows one to compare mC-1u-DNA and mC-1d-DNA to nDNA. The same sample preparation and experimental procedure was used, as described in the Methods Section. As shown in Fig. S1, the experimental results reveal that mC-1u-DNA and mC-1d-DNA are more stable than nDNA, mC-1d-DNA slightly more so than mC-1u-DNA as it exhibits a slightly higher NF value. Summarizing all experiments, mean value and standard error are in each case NF_{nDNA} = (0.557 ± 0.009), $NF_{mC\text{-}1u\text{-}DNA}$ = (0.636 ± 0.003) and $NF_{mC\text{-}1d\text{-}DNA}$ = (0.675 ± 0.008). The P-value for mC-1u-DNA (versus nDNA) is 3×10^{-3} and 6×10^{-5} for mC-1d-DNA. mC-1u-DNA and mC-1d-DNA are more stable than nDNA in contrast to mC-1c-DNA, which shows lower mechanical stability than nDNA. This suggests that effects of methylation on

the mechanical stability of dsDNA are sequence-dependent.

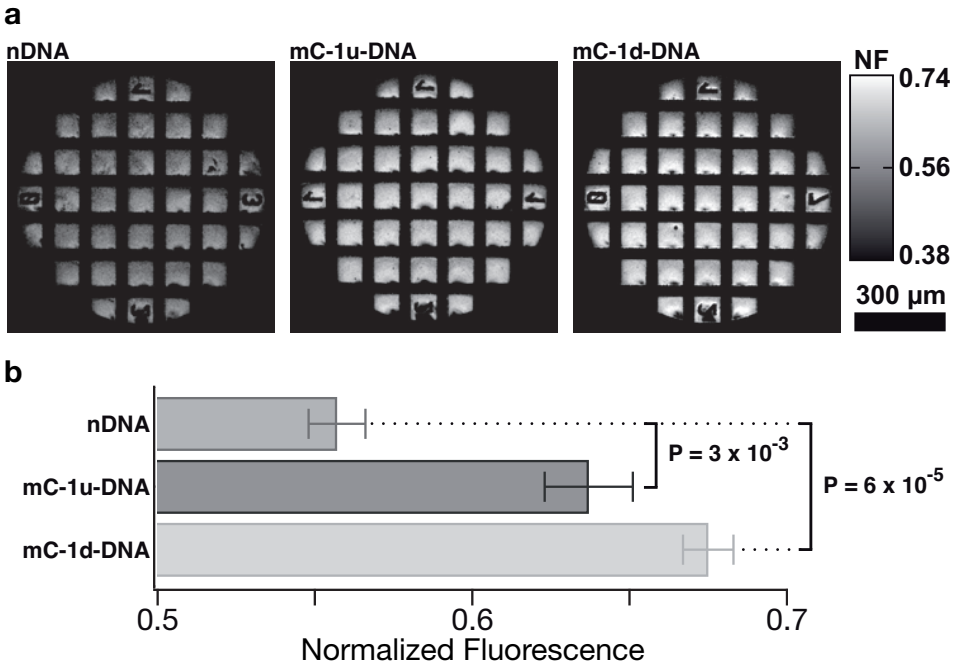

Figure S1: (a) Normalized fluorescence (NF) images of one representative experiment for nDNA, mC-1u-DNA and mC-1d-DNA. Unlike the NF signals shown in Fig. 1*b*, NF here is less homogeneous which is likely due to different pulling directions between reference and target duplex as the target duplex is pulled at the top at the 3'-end and at the bottom at the 5'-end. In case of Fig. 1*b* the duplex system was pulled at top and bottom at the 5'-ends. In comparison to nDNA (NF_{PEAK} = 0.549), mC-1u-DNA (NF_{PEAK} = 0.611) and mC-1d-DNA (NF_{PEAK} = 0.657) exhibit a higher NF, i.e., the single methylation site on each end has a stabilizing effect on the DNA duplex. (b) Analysis of 24 pads from three different experiments. mC-1u-DNA and mC-1d-DNA show a higher mean rupture force compared to non-methylated DNA (nDNA).

Determination of the mechanical stability of methylated DNA by molecular force assay measurements in unzipping geometry

Mechanical separation of the two DNA strands of a duplex in unzipping geometry provides information on the separation process that resembles helicase-induced *in vivo* strand separation. Unzipping experiments complete the picture on how methylation influences the DNA mechanics beyond what shear measurements alone reveal. We investigated the same sequence, as in shear geometry measurements, also in unzipping configuration with zero, one center and three 5-methylcytosines per strand (see Fig. S2). The DNA sequences used are listed below (**mC** represents 5-methylcytosine):

$\mathbf{1_{nDNAzip}}$, 5'-CCG AGA TAT CCG CAC CAA CG-$(T)_{20}$-$(HEGL)_5-NH_2$-3';
$\mathbf{2_{nDNAzip}}$, 5'-GGC TCT ATA GGC GTG GTT GC-$(T)_6$-T(Cy5)-$(T)_6$-CGT TGG TGC GGA TAT CTC GG-3';
$\mathbf{1_{mC-1c-DNAzip}}$, 5'-CCG AGA TAT C**mC**G CAC CAA CG-$(T)_{20}$-$(HEGL)_5-NH_2$-3';
$\mathbf{2_{mC-1c-DNAzip}}$, 5'-GGC TCT ATA GGC GTG GTT GC-$(T)_6$-T(Cy5)-$(T)_6$-CGT TGG TG**mC** GGA TAT CTC GG-3';
$\mathbf{1_{mC-3-DNAzip}}$, 5'-C**mC**G AGA TAT C**mC**G CAC CAA **mC**G-$(T)_{20}$-$(HEGL)_5-NH_2$-3';
$\mathbf{2_{mC-3-DNAzip}}$, 5'-GGC TCT ATA GGC GTG GTT GC-$(T)_6$-T(Cy5)-$(T)_6$-**mC**GT TGG TG**mC** GGA TAT CT**mC** GG-3';
$\mathbf{3_{Refzip}}$, biotin-5'-$(T)_{20}$-(Cy3)-GCA ACC ACG CCT ATA GAG CC-3'.

As shown in Fig. S2*b*, nDNA separated in unzipping geometry exhibits a NF mean value and standard error of (0.501 ± 0.002), while mC-1c-DNA exhibits the values (0.511 ± 0.003) and mC-3-DNA exhibits the values (0.583 ± 0.004). mC-1c-DNA as well as mC-3-DNA have an elevated mechanical stability compared to nDNA. The significance is characterized by a P-value of 0.017 for mC-1c-DNA versus nDNA and 1×10^{-18} for mC-3-DNA versus nDNA. In comparison to the shear configuration, where mC-1c-DNA has a destabilizing effect, mC-1c-DNA is more stable than nDNA in unzipping. The results suggest that for unzipping a DNA duplex, neighboring base pairs have a negligible effect on the methylated CpG step, since base pair by base pair is opened one after another, in contrast to the case of shear geometry, where all base pairs are under load at the same moment.

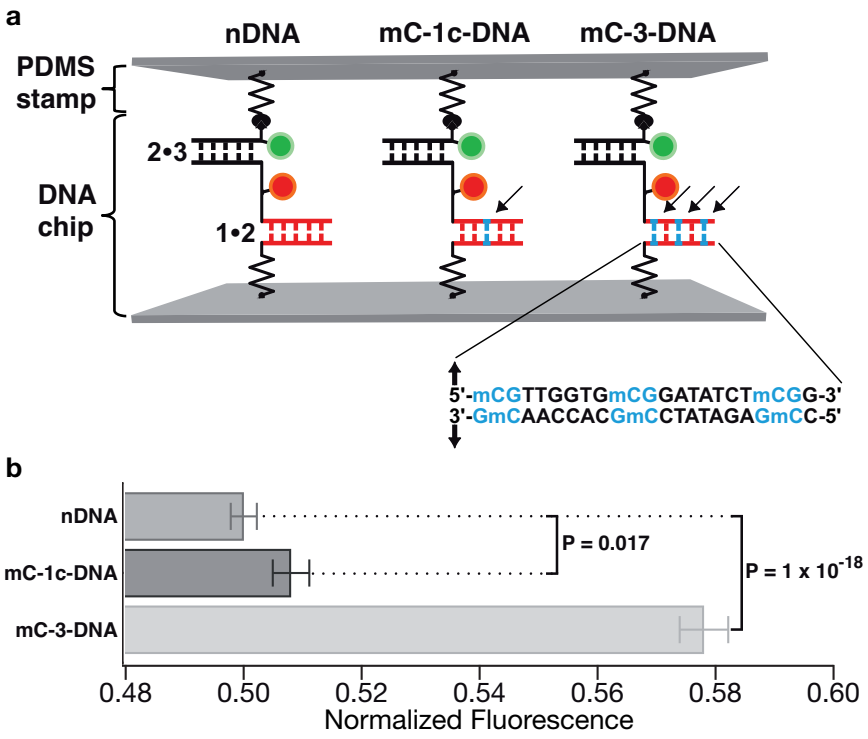

Figure S2: (a) Schematic representation of the molecular force assay in unzipping geometry. The principle of the MFA and molecular setup is the same as in Fig. 1, except that target and reference duplex are oriented such that they open like a zipper under load. The pulling velocity was 100 nm/s. (b) Analysis of 40 pads from four different experiments. mC-1c-DNA and mC-3-DNA show a higher mean rupture force than does nDNA.

SMD simulation on DNA strand separation in unzipping geometry

To visualize how methylation affects the kinetic barriers of unzipping dsDNA, we conducted SMD simulations of DNA strand separation in unzipping geometry. DNAs with the same methylation patterns (zero, one or three methylcytosines per strand) as used in shear geometry were employed. In simulations, one 3'-end of DNA was fixed, and the adjacent 5'-end was pulled. Two independent SMD simulations with 1 Å/ns-pulling velocity were performed for each DNA. A trajectory is shown in movie S5. For all simulations, we monitored the time evolution of the applied force and the number of base pairs. The results (Fig. S3) show that the mean value of applied force for rupturing mC-3-DNA is slightly larger than those of nDNA and mC-1c-DNA. Essevaz-Roulet *et al.* reported single-molecule experiments that measured the force threshold for unzipping λ DNA to be around $10 \sim 15$ pN (16). In our SMD simulations, the pulling velocity is much faster than that used in the experiments and, as expected, the force seen in our simulations is higher than in the experiment, namely is in the range 50 pN - 70 pN. The velocity dependence of the pulling force and its often negligible effect on the rupture mechanism have been described in the case of stretching proteins in (17, 18). Previous experiments have shown that the force threshold for unzipping dsDNA is sequence dependent (19). Since methylation enhances the stacking interaction between cytosine and its neighbors, it is likely that unzipping an mCG pair requires stronger force than unzipping a CG pair and, therefore, DNA with a higher methylation level is mechanically more stable than DNA with lower methylation level when stretched in the unzipping geometry.

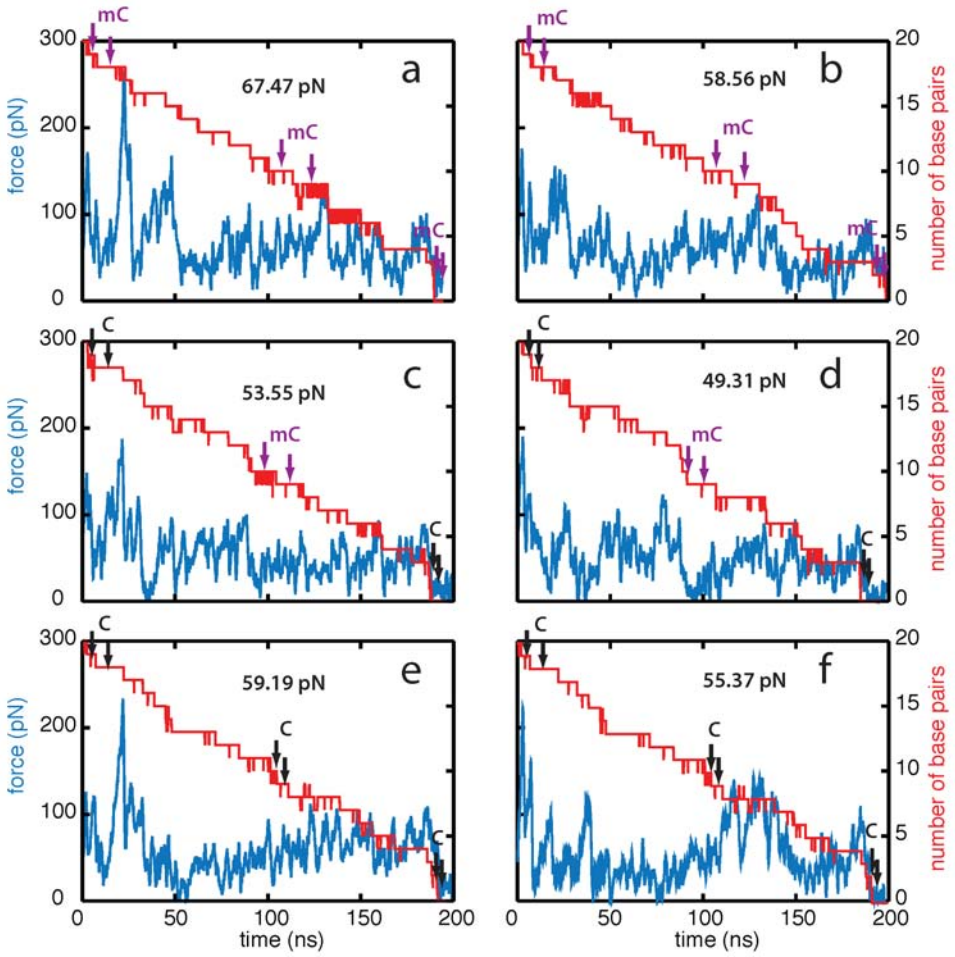

Figure S3: Time evolution of applied force (blue line) and number of base pairs (red line) as monitored in SMD simulations of unzipping mC-3-DNA (a, b), mC-1-DNA (c, d) and nDNA (e, f). Purple arrows indicate the breakage of methylated CG pairs; black arrows indicate the breakage of non-methylated CG pairs. The number given in each plot shows the mean value of force obtained from each simulation.

Supporting Movies

- **Movie S1** shows a trajectory (simulation F1, see Table 1) of strand separation of DNA stretched in shear geometry. The six methylated cytosines in DNA are indicated in yellow; the atoms subject to constraint (at bottom) and stretching force (at top) are shown in green. See Fig. 3*b*.
- **Movies S2 - S4** show trajectories of nDNA (**S2**, simulation A1), cDNA (**S3**, simulation B1) and fDNA (**S4**, simulation C1) stretched in shear geometry by steered molecular dynamics with a velocity of 1 Å/ns. The methylated cytosines in DNA are indicated in yellow; the atoms subject to constraint (at bottom) and stretching force (at top) are shown in green. See Fig. 4.
- **Movie S5** shows a simulation trajectory of strand separation of DNA stretched in unzipping geometry. The six methylated cytosines in DNA are indicated in yellow; the atoms subject to constraint and stretching force are shown in green.

Supporting Table

Name	DNA	SMD Type	Parameter	Time (ns)
A1	non-methylated (nDNA)	CVP*	1 Å/ns	118
B1	center-methylated (cDNA)	CVP	1 Å/ns	120
C1	fully-methylated (fDNA)	CVP	1 Å/ns	118
D1-D5	nDNA	CVP	10 Å/ns	8
E1-E5	cDNA	CVP	10 Å/ns	9
F1	fDNA	CVP	10 Å/ns	9
F2	fDNA	CVP	10 Å/ns	8
F3-F4	fDNA	CVP	10 Å/ns	9
F5	fDNA	CVP	10 Å/ns	8
G1	nDNA	CFP†	200 pN	90
H1	fDNA	CFP	200 pN	90

* CVP: constant velocity pulling
† CFP: constant force pulling

Table S1: List of simulations

Further supporting Figures S4 - S7

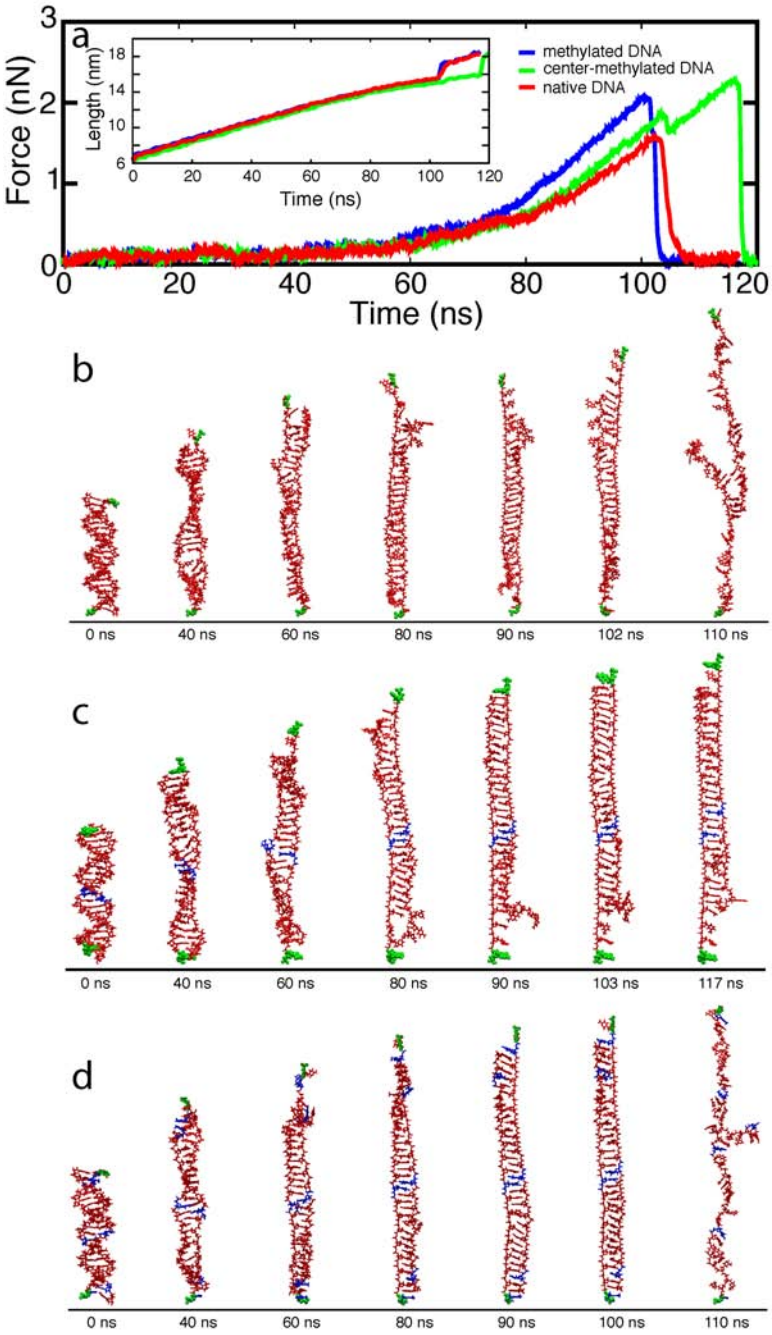

Figure S4: (a) Force and extension arising in 1 Å/ns pulling simulations. Force and extension are shown for nDNA (red), cDNA (green), and fDNA (blue) from simulations A1, B1, and C1. (b-d) Snapshots of stretched DNA. Shown are snapshots for nDNA (b), cDNA (c) and fDNA (d). The snapshots correspond to DNA conformations at 0 ns, 40 ns, 60 ns, 80 ns, 90 ns, 102 ns (force peak of nDNA) / 103 ns (minor force peak of cDNA), 117 ns (major force peak of cDNA) / 100 ns (force peak of fDNA) and 110 ns (separated strands of nDNA and fDNA). The methylated cytosines in DNA are indicated in blue; the atoms subject to constraint (at bottom) and stretching force (at top) are shown in green.

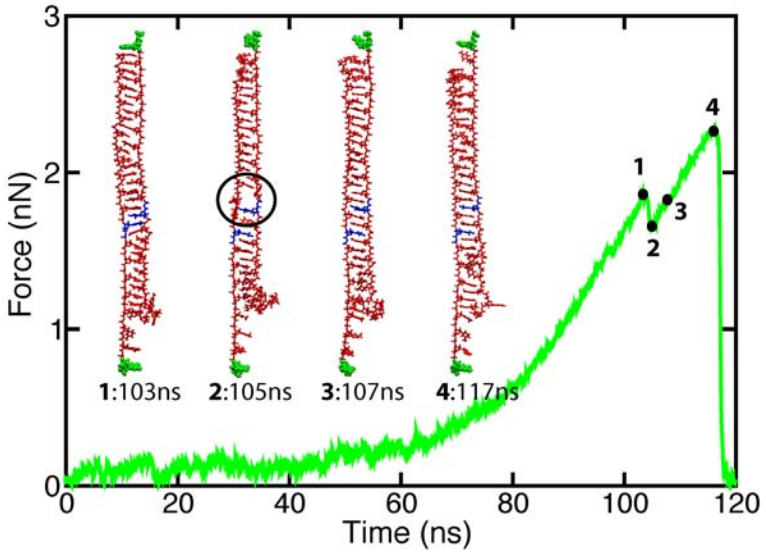

Figure S5: Snapshots of cDNA at two force peaks. The black spots on the force curve correspond to DNA conformations at 103 ns (minor force peak), 105 ns, 107 ns and 117 ns (major force peak). The black circle highlights the bubble area in DNA which results in a decrease of force at 105 ns. The methylated cytosines in DNA are indicated in blue; the atoms subject to constraint (at bottom) and stretching force (at top) are shown in green.

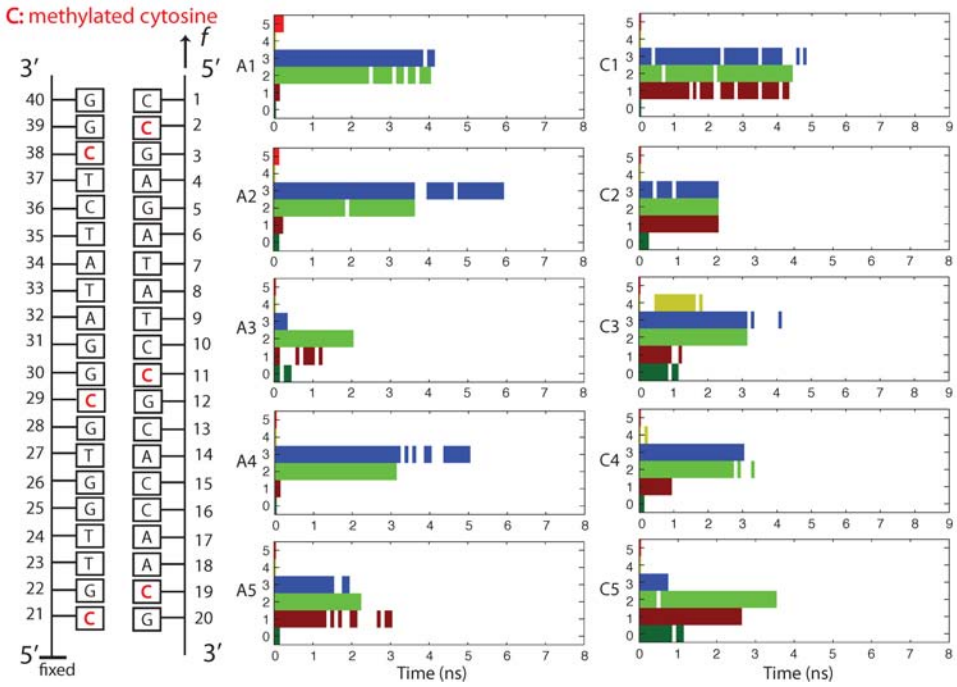

Figure S6: Progress of breaking six CG base pairs in ten 10 Å/ns pulling simulations. Shown are the analyses of nDNA (middle) and fDNA (right). Colors differentiate six different CG base pairs: (0) C21-G20; (1) G22-C19; (2) C29-G12; (3) G30-C11; (4) C38-G3; (5) G39-C2. Colors indicate that a base pairing remains intact. Schematic representation of stretched DNA is shown at left. Methylated cytosines are marked in red.

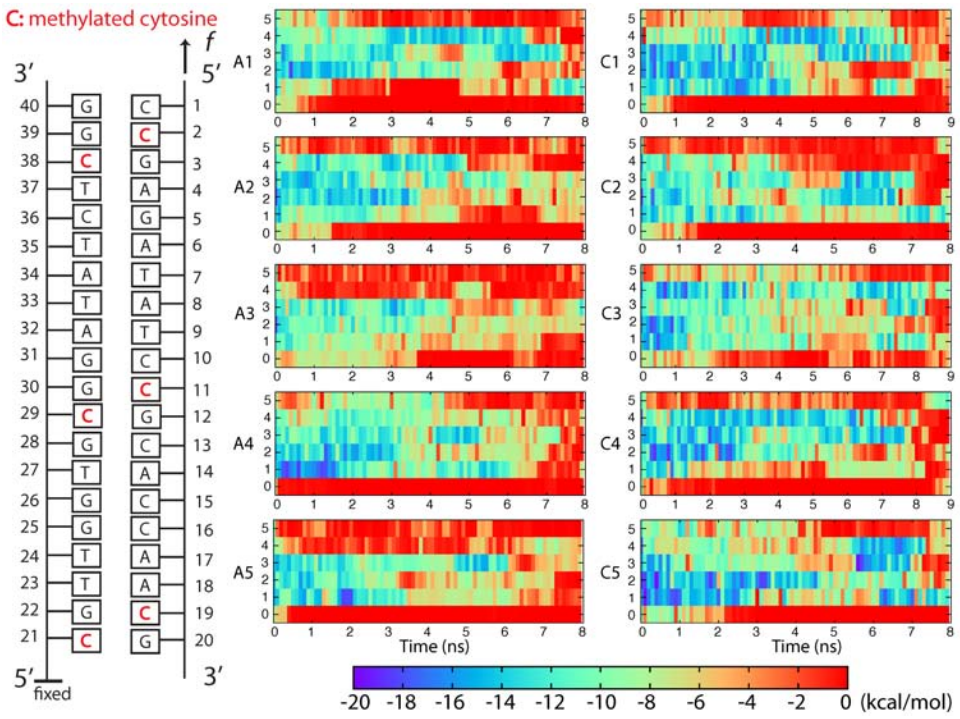

Figure S7: Time evolution of stacking energy of DNA in ten 10 Å/ns pulling simulations. Shown are the analyses of nDNA (middle) and fDNA (right). Colors indicate the value of the stacking energy of six cytosines (see color bar at bottom). The six cytosines are: (0) C21; (1) C19; (2) C29; (3) C11; (4) C38; (5) C2. Schematic representation of stretched DNA is shown at left. Methylated cytosines are marked in red.

References

1. Severin, P., Ho, D., and Gaub, H. E. (2011) A high-throughput molecular force assay for protein-DNA interactions. *Lab Chip,* **11**, 856–862.

2. Albrecht, C. H., Clausen-Schaumann, H., and Gaub, H. E. (2006) Differential analysis of biomolecular rupture forces . *J. Phys.: Condens. Matter,* **18**, 81–599.

3. Ho, D., Dose, C., Albrecht, C. H., Severin, P., Falter, K., Dervan, P. B., and Gaub, H. E. (2009) Quantitative detection of small molecule/DNA complexes employing a force-based and label-free DNA-microarray. *Biophys. J.,* **96**, 4661–4671.

4. Perutz, S., Kramer, E. J., Baney, J., and Hui, C.-Y. (1997) Adhesion between hydrolyzed surfaces of poly(dimethylsiloxane) networks. *Macromolecules,* **30**, 7964–7969.

5. Morfill, J., Kühner, F., Blank, K., Lugmaier, R. A., Sedlmair, J., and Gaub, H. E. (2007) B-S transition in short oligonucleotides. *Biophys. J.,* **93**, 2400–2409.

6. Kühner, F., Morfill, J., Neher, R. A., Blank, K., and Gaub, H. E. (2007) Force-induced DNA slippage. *Biophys. J.,* **92**, 2491–2497.

7. Neuert, G., Albrecht, C., Pamir, E., and Gaub, H. E. (2006) Dynamic force spectroscopy of the digoxigenin-antibody complex. *FEBS Lett.,* **580**, 505–509.

8. Blank, K., Morfill, J., and Gaub, H. E. (2006) Site-specific immobilization of genetically engineered variants of *Candida antarctica* lipase B. *Chembiochem,* **7**, 1349–1351.

9. Lu, X.-J. and Olson, W. K. (2003) 3DNA: a software package for the analysis, rebuilding and visualization of three-dimensional nucleic acid structures. *Nucl. Acids Res.,* **31**, 5108–5121.

10. Phillips, J. C., Braun, R., Wang, W., Gumbart, J., Tajkhorshid, E., Villa, E., Chipot, C., Skeel, R. D., Kale, L., and Schulten, K. (2005) Scalable Molecular Dynamics with NAMD. *J. Comp. Chem.,* **26**, 1781–1802.

11. MacKerell, Jr., A., Bashford, D., Bellott, M., Dunbrack, Jr., R. L., Evanseck, J., Field, M. J., Fischer, S., Gao, J., Guo, H., Ha, S., Joseph, D., Kuchnir, L., Kuczera, K., Lau, F. T. K., Mattos, C., Michnick, S., Ngo, T., Nguyen, D. T., Prodhom, B., Reiher, I. W. E., Roux, B., Schlenkrich, M., Smith, J., Stote, R., Straub, J., Watanabe, M., Wiorkiewicz-Kuczera, J., Yin, D., and Karplus, M. (1998) All-atom empirical potential for molecular modeling and dynamics studies of proteins.. *J. Phys. Chem. B,* **102**, 3586–3616.

12. Jorgensen, W. L., Chandrasekhar, J., Madura, J. D., Impey, R. W., and Klein, M. L. (1983) Comparison of Simple Potential Functions for Simulating Liquid Water. *J. Chem. Phys.,* **79**, 926–935.

13. Martyna, G. J., Tobias, D. J., and Klein, M. L. (1994) Constant Pressure Molecular Dynamics Algorithms. *J. Chem. Phys.,* **101**(5), 4177–4189.

14. Lebrun, A. and Lavery, R. (1996) Modelling extreme stretching of DNA. *Nucl. Acids Res.,* **24**, 2260–2267.

15. Albrecht, C. H., Neuert, G., Lugmaier, R. A., and Gaub, H. E. (2008) Molecular force balance measurements reveal that double-stranded DNA unbinds Under Force in Rate-Dependent Pathways. *Biophys. J.,* **94**, 4766–4774.

16. Essevaz-Roulet, B., Bockelmann, U., and Heslot, F. (1997) Mechanical separation of the complementary strands of DNA. *Proc. Natl. Acad. Sci. USA,* **94**, 11935–11940.

17. Sotomayor, M. and Schulten, K. (2007) Single-Molecule Experiments in Vitro and in Silico. *Science,* **316**, 1144–1148.

18. Lee, E. H., Hsin, J., Sotomayor, M., Comellas, G., and Schulten, K. (2009) Discovery through the computational microscope. *Structure,* **17**, 1295–1306.

19. Rief, M., Clausen-Schaumann, H., and Gaub, H. E. (1999) Sequence-dependent mechanics of single DNA molecules. *Nat. Struct. Biol.,* **6**, 346–349.